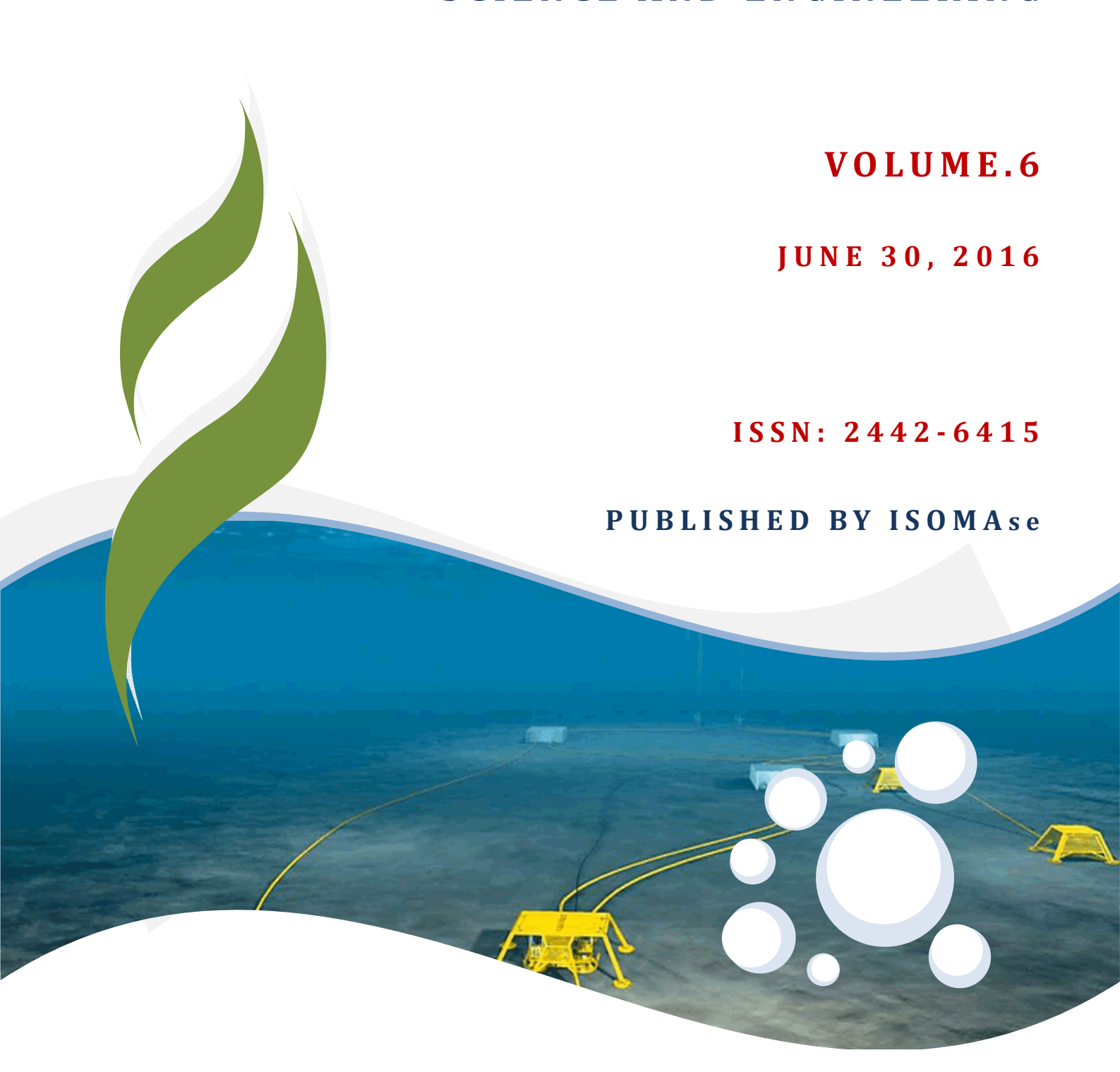
JOURNAL OF SUBSEA AND OFFSHORE

SCIENCE AND ENGINEERING



Journal of Subsea and Offshore

-Science and Engineering-

Vol.6: June 30, 2016

Contents

About JSOse Scope of JSOse Editors

Title and Authors				
Subsea Pipeline Analysis of Nosong-Bongawan Field, Malaysia				
Nurul Nabila, Mukminah, Muhammed Amirul Asyraf, Fahd Ezadee, J.Koto				
The Effect of Flat Plate Theory Assumption in Post-Stall Lift and Drag				
Coefficients Extrapolation with Viterna Method				
Faisal Mahmuddin				
Review on Roncador Field Production and Gas Lift Pipelines				
Adibah Fatihah.M.Y, Noor Zairie. M, Nur Ain.A.R, Nursahliza. M.Y, J.Koto	14 - 21			

ISOMAse

Journal of Subsea and Offshore -Science and Engineering-

Vol.6: June 30, 2016

About JSOse

The **Journal of Subsea and Offshore -science and engineering- (JSOse),** ISSN's registration no: 2442-6415 is an online professional journal which is published by the International Society of Ocean, Mechanical and Aerospace -scientists and engineers- (ISOMAse), Insya Allah, four volumes in a year which are March, June, September and December.

The mission of the JSOse is to foster free and extremely rapid scientific communication across the world wide community. The JSOse is an original and peer review article that advance the understanding of both science and engineering and its application to the solution of challenges and complex problems in subsea science, engineering and technology.

The JSOse is particularly concerned with the demonstration of applied science and innovative engineering solutions to solve specific subsea and offshore industrial problems. Original contributions providing insight into the use of computational fluid dynamic, heat transfer, thermodynamics, experimental and analytical, application of finite element on offshore and subsea, offshore structural and impact mechanics, stress and strain localization and globalization, metal forming, behaviour and application of advanced materials in shallow and deepwater, shallow and deepwater installation challenges, vortex shedding, vortex induced vibration and motion, flow assurance, ultra-deepwater drilling riser, wellhead integrity and soon from the core of the journal contents are encouraged.

Articles preferably should focus on the following aspects: new methods or theory or philosophy innovative practices, critical survey or analysis of a subject or topic, new or latest research findings and critical review or evaluation of new discoveries.

The authors are required to confirm that their paper has not been submitted to any other journal in English or any other languages.

ISOMAse

International Society of Ocean, Mechanical and Aerospace -Scientists and Engineers-

Journal of Subsea and Offshore -Science and Engineering-

Vol.6: June 30, 2016

Scope of JSOse

JSOse welcomes manuscript submissions from academicians, scholars, and practitioners for possible publication from all over the world that meets the general criteria of significance and educational excellence. The scope of the journal is as follows:

- Shallow, Deep and Ultra-deep Water and Arctic Pipelines and Offshore Structure
- Shallow, Deep, Ultra-deep Water Installation Challenges
- Subsea and Offshore Challenges in Pipe Materials, Flow Assurance, Multi Phases Flow, Equipment and Hardware
- Flexible Pipe and Umbilical
- Riser, Mooring Lines Design and Mechanics System
- Advanced Engineering, Lateral and Upheaval Buckling, Pipeline Soil Interactions
- Challenges of High Pressure High Temperature (HPHT) in Ultra-deep Water
- Vortex Shedding and Vibration Suppression (VIV & VIM)
- Project Experiences, Case Study and Lessons Learned on Subsea and Offshore
- Integration of Management, Materials, Safety and Reliability
- Certified Verification Analysis (CVA)
- Subsea and Offshore Structures Construction.

The International Society of Ocean, Mechanical and Aerospace –science and engineering is inviting you to submit your manuscript(s) to isomase.org@gmail.com for publication. Our objective is to inform the authors of the decision on their manuscript(s) within 2 weeks of submission. Following acceptance, a paper will normally be published in the next online issue.

ISOMAse

Journal of Subsea and Offshore

-Science and Engineering-

Vol.6: June 30, 2016

Editors

Chief-in-Editor

Jaswar Koto (Ocean and Aerospace Research Institute, Indonesia)

Associate Editors

Radzuan Junin

Ab. Saman bin Abd. Kader (Universiti Teknologi Malaysia, Malaysia)

Adhy Prayitno (Universitas Riau, Indonesia)

Adi Maimun bin Abdul Malik (Universiti Teknologi Malaysia, Malaysia)
Ahmad Fitriadhy (Universiti Malaysia Terengganu, Malaysia)

Ahmad Zubaydi (Institut Teknologi Sepuluh Nopember, Indonesia)
Bambang Purwohadi (The Institution of Engineers Indonesia, Indonesia)

Carlos Guedes Soares (University of Lisbon, Portugal)
Harifuddin (DNV, Batam, Indonesia)
Hassan Abyn (Persian Gulf University, Iran)
Mohamed Kotb (Alexandria University, Egypt)

Moh Hafidz Efendy (PT McDermott, Indonesia)
Mohd Nasir Tamin (Universiti Teknologi Malaysia, Malaysia)
Mohd Yazid bin Yahya (Universiti Teknologi Malaysia, Malaysia)
Mohd Zaidi Jaafar (Universiti Teknologi Malaysia, Malaysia)
Musa Mailah (Universiti Teknologi Malaysia, Malaysia)
Priyono Sutikno (Institut Teknologi Bandung, Indonesia)

Rudi Walujo Prastianto (Institut Teknologi Sepuluh Nopember, Indonesia)

(Universiti Teknologi Malaysia, Malaysia)

Sergey Antonenko (Far Eastern Federal University, Russia) Sunaryo (Universitas Indonesia, Indonesia)

Sutopo (PT Saipem, Indonesia)

Tay Cho Jui (National University of Singapore, Singapore)
Wan Rosli Wan Sulaiman (Universiti Teknologi Malaysia, Malaysia)
Zahiraniza Mustafa (Universiti Teknologi Petronas, Malaysia)

Yasser Mohamed Ahmed (Alexandria University, Egypt)

ISOMAse

Subsea Pipeline Analysis of Nosong-Bongawan Field, Malaysia

Nurul Nabila, Mukminah, Muhammed Amirul Asyraf, Fahd Ezadee, and J.Koto, A,*

Paper History

Received: 3-June-2016

Received in revised form: 28-June-2016

Accepted: 30-June-2016

ABSTRACT

The Nosong-Bongawan North field is located in Block B310 in Offshore Sabah Area, approximately 75km North of Labuan and approximately 30km North of SUPG-B, Malaysia. This paper discussed subsea pipeline of the Nosong-Bongawan field development using Subsea Pro Simulation to determine wall thickness and stress and ANSYS to determine the deformation due to buckling of pipeline. Simulation results were compared with the actual operating data.

KEY WORDS: Nosong-Bongawan North Field, Subsea Pipeline, Stress, Wall Thickness, Buckling, Deformation.

NOMENCLATURE

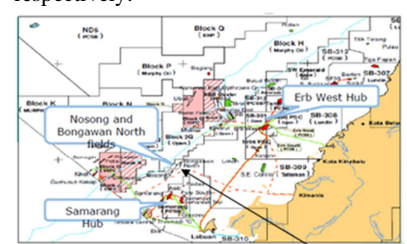
WHP Wellhead Platform

MMSCFD Million standard cubic feet of gas per day

1.0 INTODUCTION

The Nosong-Bongawan North field is located in Block B310 in Offshore Sabah Area, approximately 75km North of Labuan and approximately 30km North of SUPG-B. PETRONAS is currently undertaking the development of this field. The business target of the Nosong-Bongawan Gas Development is to deliver 50 MMSCFD production to SUPG-B, and ultimately to LGAST. The Nosong and Bongawan fields are at 90m and 95m water depth

respectively.



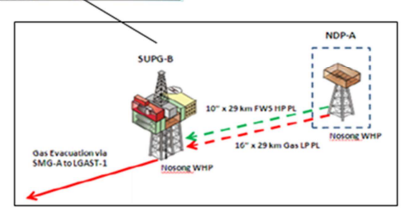


Figure.1: Nosong-Bongawan field development.

This paper attempted to develop a comprehensive subsea development plan for the Nosong field. The subsea development encompasses all the processes required to transport the gas from the well to the pre-processing facility located on the NDP-A bottom-founded platform. After that, this project will address the piping requirements to transport the gas from the NDP-A platform to the SUPG-B platform

2.0 DEVELOPMENT OF NOSONG FIELD

2.1 Overall Overview of Nosong Field

PETRONAS undertakes the development of Nosong North field which is located in Block B310 in Sabah Area, approximately 75km North of Labuan and approximately 30km North of Sumandak Central Processing Platform (SUPG-B CPP). As described in the previous scope section, this report covers only the bottom-founded platform (fixed platform) and so the selection

^{a)} Department of Aeronautic, Automotive and Ocean Engineering, Faculty of Mechanical Engineering, Universiti Teknologi Malaysia

b) Ocean and Aerospace Engineering Research Institute, Indonesia

^{*}Corresponding author: jaswar@utm.my and jaswar.koto@gmail.com

is shallow water area (75 km) to the onshore.

Nosong Gas Development facilities hub scopes are comprised of following:

- One (1) Wellhead Platform (WHP).
- Two (2) dedicated new trunk lines; 10-inch FWS (High Pressure); approximately 30km from WHP to existing SUPG-B.
- Offshore modification and tie-in WORKS at existing SUPG-B

2.2 Nosong Field Development

2.2.1 Business Target of Production

The business target by the stakeholders of this Nosong Gas Development project is to deliver **50 MMSCFD** production by **June 2017** to SUPG-B CPP, and ultimately to Labuan Gas Terminal (LGAST). The Nosong field is at 90m water depth.

2.2.2 Specific Location of Field

From exploration and the field study, the location (geodetic data) of the field is furnished by them is as table follow. The geodetic data for the offshore pipelines are referenced to Universal Transverse Mercator (UTM) local projection with Timbalai 1948 local datum.

Table.1: Datum and local projection info.

Local Datum	Detail Information				
Datum	Timbalai 1948				
Spheroid	Everest 1830 (1967 Def)				
Semi-major axis	6 377 298.556 m				
Semi-minor axis	6 356 097.550 m				
Inverse flattening	300.8017				

Local Projection	Detail Information				
Map projection	UTM Zone 50°N				
Grid projection	Universal Transverse Mercator				
Latitude of origin	00° 00' 00" N				
Longitude of origin	117° 00' 00" E				
False Easting at origin	500 000 m				
False Northing at origin	0 m				
Scale factor at origin	0.9996				

2.2.3 Regulation, Design Codes and Standard

The design of the pipeline system in order of priority are conformance with the requirements of the PETRONAS Technical Standards (PTS) and international codes and standards as specified in PTS, unless specified otherwise.

If the Government or Local Authority Laws and Regulations are more stringent than the PTS, the former takes precedence. Deviations from these standards shall be agreed upon and

approved by Petroliam Nasional Bhd. For any deviation/conflict from applicable rules, codes and standards, the prevailing priorities will be according to following sequence:

- PETRONAS Technical Standards (PTS)
- National or Local Rules and Regulations
- International Codes (API, ANSI, AISC, ASME, DNV and ISO)

As for pipeline, the primary code for the design of the pipeline and riser systems shall be in accordance with PTS 31.40.00.20, September 2012 Rev 0, 'Pipeline and Riser Engineering' and its supplementary documents.

2.2.4 Malaysian Government, Local Authority Laws and Regulation

The field development was governed by the below government and local authority laws and regulations as follows:

- Petroleum (Safety Measures) Act 302, 1984 (incorporating all amendments up to 1 January 2006)
- Petroleum (Safety Measures) (Transportation of Petroleum by Pipeline) Regulation, 1985, PU(A) 85/1985
- Department of Occupational Safety and Health (DOSH), Malaysia

2.3 Standard and Specifications

2.3.1 PETRONAS Technical Specifications (PTS)

The specification of the platform shall be complying with the PTS.

Table.2: PTS standards

No of PTS	Specification
PTS 1.40.00.20	Pipeline and Riser Engineering, September 2012
PTS 1.40.10.10 PTS 0.10.73.33	Riser Design, October 2011 Installation and Commissioning of Cathodic Protection Systems, October 2011
PTS 30.10.73.34	Design of Cathodic Protection Systems for Offshore Pipelines (Amendments/Supplements to DNV RP F103), April 2012
PTS 30.48.00.31	Protective Coatings and Linings, September 2012
PTS 31.40.20.33	Linepipe Induction Bends (Amendments/supplements to ISO 15590-1), August 2012
PTS 31.40.20.38	Linepipe Specification (Amendments/supplements to API 5L 44th Edition / ISO 3183:2007), October 2011
PTS 31.40.21.30	Pipeline Fittings (Amendments/Supplements to ISO 15590-2), January 2010
PTS 31.40.00.20	Pipeline and Riser Engineering, September 2012
PTS 31.40.10.10	Riser Design, October 2011
PTS 30.10.73.33	Installation and Commissioning of Cathodic Protection Systems, October 2011
PTS 30.10.73.34	Design of Cathodic Protection Systems for Offshore Pipelines (Amendments/Supplements to DNV RP F103), April 2012
PTS 30.48.00.31	Protective Coatings and Linings, September 2012
PTS 31.40.20.33	Linepipe Induction Bends (Amendments/supplements to ISO 15590-1), August

	2012
PTS 31.40.20.38	Linepipe Specification (Amendments/supplements to API 5L 44th Edition / ISO 3183:2007), October 2011
PTS 31.40.21.30	Pipeline Fittings (Amendments/Supplements to ISO 15590-2), January 2010
PTS 31.40.21.34	Carbon and Low Alloy Steel Pipeline Flanges for Use in Oil and Gas Operations (Amendments/Supplements to MSS SP-44), September 2012
PTS 31.36.00.30	Pipeline Transportation Systems – Pipeline Valves (Amendments / Supplements to API Spec 6D/ISO 14313), September 2012
PTS 31.40.10.13	Design of Pipeline Pig Trap Systems, November 2010
PTS 31.40.30.30	Concrete Coating of Linepipe, January 2011
PTS 31.40.30.31	External Polyethylene and Polypropylene Coating for Linepipe, January 2010
PTS 31.40.30.32	External Fusion Bonded Epoxy Powder Coating for Linepipe, September 2012
PTS 31.40.30.33	Bituminous Enamel Coating of Steel Linepipe, October 2011
PTS 31.40.30.36	Elastomer Coatings and Monel Sheating for Offshore Riser Protection, October 2012
PTS 31.40.40.38	Hydrostatic Pressure Testing of New Pipelines, September 2012
PTS 31.40.50.30	Pre-commissioning of Pipelines, January 2010
PTS 61.40.20.30	Welding of Pipelines and Related Facilities (Amendments/Supplements to ANSI/API STD 1104), October 2011

2.3.2 Industry Codes and Standards

Besides PTS, the field also shall in conformance with API and ASME as shown in Table.3 and Table.4, respectively.

2.3.2.1 American Petroleum Institute (API)

Table.3: API specification

Table.5: AFT specification					
API	Description				
API RP 1111	Design, Construction, Operation and Maintenance of Offshore Hydrocarbon Pipelines, May 2011				
API Spec 5L	Specification for Line Pipe, 45th Edition, December 2012				
API Spec 6D	Specification for Pipeline Valves, October 2012				
API Std 1104	Welding of Pipelines and Related Facilities, 21st Edition, September 2013				

2.3.2.2 American Society of Mechanical Engineers (ASME)

Table.4: ASME specification

ASME	Description
ASME VIII Div. 1	Rules of Construction of Pressure Vessel, July 2013
ASME B31.8	Gas Transmission and Distribution Piping Systems, January 2013
ASME B16.5	Pipe Flanges and Flanged Fittings, April 2013
ASME B16.9	Factory-Made Wrought Butt Welding Fittings, February 2013
ASME B16.20	Metallic Gasket for Pipe Flanges – Ring-Joint, Spiral-Wound, and Jacketed, June 2013
ASME B36.10M	Welded and Seamless Wrought Steel Pipe, 2010

2.3.3 Water Depth

The water depths at the offshore facilities/platforms are presented in Table.5 below and are taken from Nosong WHP (NDP-A) to Sumandak (SUPG-B CPP) Pipeline route.

Table.5: Water Depths at Facilities

Location	Approximate Water Depth wrt. Mean Sea Level (m)
NDP-A	89.3
SUPG-B	42.81

The water depths along the proposed pipeline routes from Nosong WHP to Sumandak SUPG-B are presented in Table 4.5 below and are taken from Nosong WHP to Sumandak SUPG-B Pipeline route survey information (which is not covered in this report).

Table.6: Maximum and Minimum Water Depth along Pipeline Routes

Pipeline	Water Depth wrt. MSL (m)				
	Minimum	Maximum			
16-inch NAG LP Pipeline from NDP-A to SUPG-B	36.82	89.27			

2.3.4 Tidal and Surge Data

The tidal and surge data to be used for wellhead, manifold and pipeline design and riser at NDP-A platform are extracted from Nosong Bongawan Metocean Criteria. The tidal and surge data to be used for riser design at existing SUPG-B are extracted from Metocean Criteria at Sumandak Tepi and Sumandak Selatan as shown in Table.7:

Table.7: Tidal and Surge data for Nosong field and compared also with Sumandak Tepi and Sumandak Selatan area

Criteria	Nosong Bongawan	Sumandak Tepi & Sumandak Selatan
Highest Astronomical Tide (m)	0.94	1.23
Mean Sea Level (m)	0	0
Lowest Astronomical Tide (m)	-1.17	-0.97
1 Year Storm Surge (m)	0.3	0.3
100 Year Storm Surge (m)	0.6	0.6

2.3.5 Wave Data

The wave data to be used for pipeline design and riser at NDP-A platform are as given in Table.8 and Table.9 and are extracted from Nosong Bongawan Metocean Criteria.

Table.8: Wave criteria for return period of 1 year

Direction	Omni	N	NE	E	SE	S	SW	W	NW
$\mathbf{H}_{s}\left(\mathbf{m}\right)$	3.9	3.9	3.2	1.6	2	2	2.7	3.1	3.5
T _p (sec)	9.7	9.7	8.8	6.3	6.9	7	8.1	8.6	9.2
$\mathbf{H}_{\max}\left(\mathbf{m}\right)$	6.8	6.8	5.7	3	3.6	3.7	4.9	5.5	6.2
T _{ass} (sec)	9	9	8.2	5.9	6.4	6.5	7.6	8	8.5

Table.9: Wave criteria for return period of 10 years

Direction	Omni	N	NE	E	SE	S	SW	W	NW
$\mathbf{H}_{\mathrm{s}}\left(\mathbf{m}\right)$	4.6	4.6	3.9	2.0	2.4	2.4	3.3	3.7	4.2
T _p (sec)	10.6	10.6	9.7	6.9	7.6	7.7	8.9	9.4	10.0
$\mathbf{H}_{\max}\left(\mathbf{m}\right)$	8.1	8.1	6.8	3.6	4.3	4.4	5.9	6.5	7.3
T _{ass} (sec)	9.8	9.8	9.0	6.4	7.1	7.2	8.3	8.8	9.3

2.3.6 Current Data

The current data to be used for project development especially for pipeline design and riser at NDP-A platform are as given in Table.10 and Table.11 which are extracted from Nosong Bongawan Metocean Criteria.

Table.10: Current data for return period 1 year

Direction	<u>Omni</u>	N	<u>NE</u>	<u>E</u>	SE	<u>S</u>	<u>SW</u>	W	<u>NW</u>
At surface (1.0D) (cm/s)	114	71	114	74	53	64	82	74	51
Mid Depth (0.5D) (cm/s)	91	57	91	59	42	51	65	59	40
Near ottom (0.1D) (cm/s)	53	33	53	34	25	30	38	34	24

Table.11: Current data for return period 10 years

Direction	Omni	N	NE	E	SE	S	SW	W	NW
At surface (1.0D) (cm/s)	143	89	143	93	67	80	103	93	64
Mid Depth (0.5D) (cm/s)	114	71	114	74	53	64	82	74	51
Near ottom (0.1D) (cm/s)	67	42	67	43	31	37	48	43	30
Near Seabed (0.01D) (cm/s)	31	19	31	20	14	17	22	20	14

Notes

At other water depths not specified above, the current velocities shall follow the 1/7th rule. The formula is as below:

$$V_z = V_d \cdot \left(\frac{z}{d}\right)^{1/7} \tag{1}$$

Where, d is total water depth, z is depth of interest above seabed, V_z is current speed at depth 'z' metres and V_d is current speed at the surface

2.3.7 Seawater Properties

The seawater properties are presented in Table.12

Table.12: Sea Water Properties

	Parameters	Values
	Density	1025 kg/m^3
Sea	Kinematic Viscosity	0.96 x 10 ⁻⁶ m ² /s (At 25°C)
Water	Mean Surface Temperature	28.5 °C
	Mean Seabed Temperature	21.1 °C

2.3.8 Marine Growth

In the absence of more accurate data, the marine growth thickness for the risers is considered to be 90mm at Mean Sea Level. Marine growth is assumed to decrease by 1mm for every 2m of water depth. The Marine growth density is 1025 kg/m³.

2.3.9 Soil Properties

The soil properties along the proposed pipeline route are extracted from the Nosong WHP to Sumandak SUPG-B Pipeline Route Survey Report. The soil properties with respect to KP as

summarized below.

Table.13: Nosong WHP to Sumandak SUPG-B Pipeline Route Soil Properties

Soil Proper	Soil Properties					
Kilometer Point	Drop Core	Soil Type	Su (kPa)			
0 - 0.5	DC-1.0	Very loose SAND with shell fragments	N/A			
0.5 - 1.5	DC-2.0	Very loose SAND with shell fragments	N/A			
1.5 - 2.5	DC-3.0	Very loose SAND with shell fragments	N/A			
2.5 - 3.5	DC-4.0	Very loose SAND with shell fragments	N/A			
3.5 - 4.5	DC-5.0	Very loose clayey SAND with shell fragments	N/A			
4.5 - 5.5	DC-6.0	Very loose clayey SAND with shell fragments	N/A			
5.5 - 6.5	DC-7.0	Very loose clayey SAND with shell fragments	N/A			
6.5 - 7.5	DC-8.0	Soft grey sandy CLAY with shell fragments	14			
7.5 - 8.5	DC-9.0	Very soft grey sandy CLAY with shell fragments	11			
8.5 - 9.5	DC-10.0	Soft grey sandy CLAY with shell fragments	12.5			
9.5 - 10.5	DC-11.0	Very soft grey sandy CLAY with shell fragments	5			
10.5- 11.5	DC-12.0	Very soft grey sandy CLAY with shell fragments	7			
11.5 - 12.5	DC-13.0	Very soft grey sandy CLAY with shell fragments	7			
12.5 - 13.5	DC-14.0	Very soft grey sandy CLAY with shell fragments	9			
13.5 - 14.5	DC-15.0	Very soft grey sandy CLAY with shell fragments	9			
14.5 - 15.5	DC-16.0	Very soft grey sandy CLAY with shell fragments	5			
15.5 - 16.5	DC-17.0	Very soft grey sandy CLAY with shell fragments	5			
16.5 - 17.5	DC-18.0	Very soft grey sandy CLAY with shell fragments	7			
17.5 - 18.5	DC-19.0	Very soft grey sandy CLAY with shell fragments	3			
18.5 - 19.5	DC-20.0	Very soft grey sandy CLAY with shell fragments	5			
19.5 - 20.5	DC-21.0	Very soft grey sandy CLAY with shell fragments	5			
20.5 - 21.5	DC-22.0	Very soft grey sandy CLAY with shell fragments	6			
21.5 - 22.5	DC-23.0	Very soft grey sandy CLAY with shell fragments	7			
22.5 - 23.5	DC-24.0	Very soft grey sandy CLAY with shell fragments	8			
23.5 - 24.5	DC-25.0	Very soft grey sandy CLAY with shell fragments	3			
24.5 - 25.5	DC-26.0	Very soft grey sandy CLAY with shell fragments	4			

25.5 - 26.5	DC-27.0	Very soft grey sandy CLAY with shell fragments	5
26.5 - 27.5	DC-28.0	Very soft grey sandy CLAY with shell fragments	10
27.5 - 28.5	DC-29.0	Very soft grey sandy CLAY with shell fragments	3
28.5 - 29.5	DC-30.0	Very soft grey sandy CLAY with shell fragments	6
29.5 - 30.5	DC-31.0	Very soft grey sandy CLAY with sheTestll fragments	6
30.5 - 31.5	DC-32.0	Very soft grey sandy CLAY with shell fragments	6
31.5 - 31.9	DC-33.0	Very soft grey sandy CLAY with shell fragments	4

The soil geotechnical properties along the pipelines are taken from Laboratory Test of Nosong WHP to Sumandak SUPG-B Pipeline Route Survey (Ref. 10) and are summarised below.

Table.14: Nosong WHP to Sumandak SUPG-B Pipeline Route Soil Properties

Drop Core	Depth	Water Content	Wet Density	Dry Density
	(m)	(%)	(Mg/m ³)	(Mg/m ³)
DC-1.0	0.8	40	1.95	1.39
DC-2.0	0.8	40	1.92	1.37
DC-3.0	0.8	40	1.92	1.37
DC-4.0	0.8	39	1.95	1.4
DC-5.0	0.72	39	1.95	1.4
DC-6.0	0.72	39	1.95	1.4
DC-7.0	0.77	37	1.95	1.42
DC-8.0	0.8	40	1.92	1.37
DC-9.0	0.3	33	1.83	1.38
DC-10.0	0.3	33	1.83	1.38
DC-11.0	0.3	35	1.83	1.36
DC-12.0	0.3	35	1.83	1.36
DC-13.0	0.4	40	2.29	1.64
DC-14.0	0.4	41	1.94	1.38
DC-15.0	0.4	32	2.03	1.54
DC-16.0	0.4	30	2.06	1.58
DC-17.0	0.4	36	2.01	1.48
DC-18.0	0.4	35	2	1.48
DC-19.0	0.4	34	2	1.49
DC-20.0	0.4	42	1.91	1.35
DC-21.0	0.2	21	1.84	1.52
DC-22.0	0.4	34	2.05	1.53

DC-23.0	0.4	46	1.91	1.31
DC-24.0	0.4	34	1.99	1.49
DC-25.0	0.4	35	1.99	1.47
DC-26.0	0.3	38	1.89	1.37
DC-27.0	0.3	38	1.7	1.23
DC-28.0	0.2	42	1.93	1.36
DC-29.0	0.4	45	1.8	1.24
DC-30.0	0.3	38	1.7	1.23
DC-31.0	0.3	38	1.7	1.23
DC-32.0	0.2	40	1.87	1.34
DC-33.0	0.2	39	1.87	1.35

3.0 SUBSEA PIPELINE ANALYSIS

3.1 Pipeline Design Parameter

The pipeline design and calculation is the most crucial part in any subsea field development process. The parameters will be taken into consideration in this work are: structure of pipe, weight of pipe, design pressure and pipeline stress.

The pipeline design and operational data is based upon Pipeline Steady State Hydraulic Analysis Report and Corrosion Design Basis Memorandum is presented in Table.15. The hydrostatic test pressure shall be 1.5 times maximum allowable operating pressure / design pressure of the pipeline system or the pressure that produces hoop stress in the weakest component equal to 90% of SMYS, whichever is smaller. In the event of pig stuck during pigging operation, it is anticipated that the riser and spool at NDP-A side may be exposed to a build-up of topside pressure. Therefore, all flanges at NDP topside, riser and spool has been rated to NDP-A topside pressure and the NDP-A riser and spool has been designed to withstand NDP-A topside pressure.

 Table.15: Pipeline Design and Operating Data

	ie Besign and Operati	-6
Parameter	10-inch FWS HP Pipeline from NDP-A to SUPG-B	16-inch NAG LP Pipeline from NDP-A to SUPG- B
Flow Medium	FWS	NAG
Min. Product Density (kg/m³)	117.68	14.64
Max. Product Density	266.68	41.49
(kg/m³)		
Internal Corrosion Allowance (mm)	3	3
Corrosion Allowance for Riser Splash zone (including external) (mm)	6	6
Outside Diameter (mm)	273	406.4
Design Pressure for NDP-A Topside, Riser and Spool (bar)	186.2	186.2

	sure for Subsea PG-B Topside, (bar)	137.9	82.74	
Hydrotest P Pipeline Sys	ressure for	206.85	124.11	
Max. Design Temperature		80	80	
(°C)				
Min. Design	Temperature	0	0	
(°C)				
Maximum (Temperatur		68	64	
Pipeline and (vears)	Riser Design Life	25	25	
Linepipe Type		Н	FW	
Material Grade for Linepipe		API 5L		
NDP-A Topside Rating		1500	1500	
Subsea Flange Rating		1500	1500	
SUPG-B To System Rati	pside and Pipeline ng	900	600	
	Above Splashzone	1mm thk. Glass Flake Filled Polyester	1mm thk. Glass Flake Filled Polyester	
Proposed External	Riser Splashzone	12.7mm thk. Neoprene over 0.5mm thk. FBE	12.7mm thk. Neoprene over 0.5mm thk. FBE	
Anti- Corrosion Coating	Submerged Risers and Bends	0.5mm thk. FBE	0.5mm thk. FBE	
	Subsea Pipeline	5.5mm thk. AE with Concrete Weight Coating	5.5mm thk. AE with Concrete Weight Coating	

3.2 Pipeline Material and Steel Properties

The material thermal properties and densities of the pipelines and risers are shown in Table.16.

Table.16: Material Thermal Properties and Densities

Coating Type	Density	Thermal Conductivity
	(kg/m3)	(W/m.K)
Asphalt Enamel (AE)	1280	0.69
Fusion Bonded Epoxy (FBE)	1400	0.3
3 Layer Polyethylene (3LPE)	925	0.6
3 Layer Polypropylene (3LPP)	900	0.22
Concrete Coating	3044	2.1
Carbon Steel Pipe	7850	45.35
Neoprene Coating	1450	0.265

-Science and Engineering-, Vol.1

The design will be based on the following steel material properties shown in Table.17.

Table.17: Steel Properties

Description	Unit	Value
Young's Modulus, E	MPa	207000
Poisson's Ratio,	-	0.3
Coefficient of Thermal Expansion	°C	11.7 x 10-6

4.0 SUBSEA STRENGTH ANALYSIS

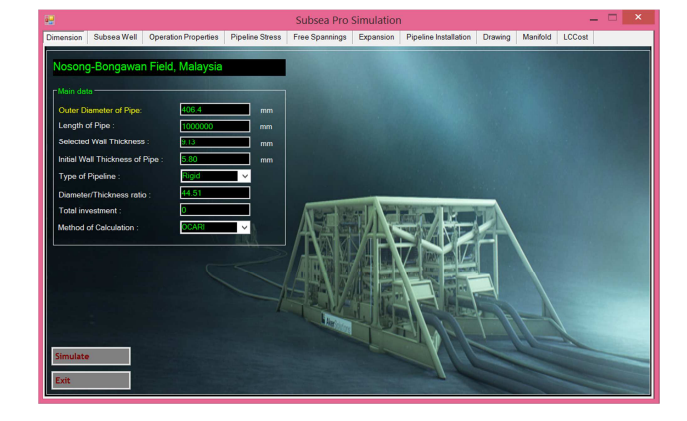
3.1 Pipeline Design Parameter

The pipeline analysis is carried out using Subsea Pro Simulation to determine wall thickness and ANSYS to determine total deformation during operation. The pipeline is subjected to internal pressure and hydrostatic pressure.

Table 18 and Figure.2 show wall thickness and stress analysis using Subsea Pro Simulation. The simulation result shows very close to the actual wall thickness.

Table.18: Actual and simulation result wall thicknesses.

	Actual	Subsea Pro Simulation
Wall Thickness (mm)	9.525	9.130



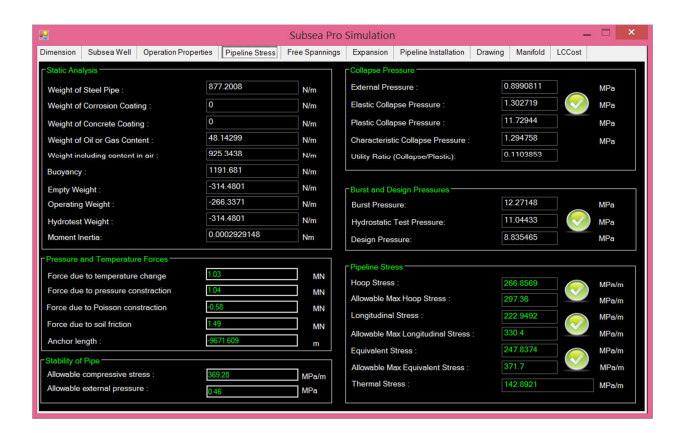


Figure.2: Wall thickness and stress analysis using Subsea Pro Simulation.

Two types of analysis were carried out, the first is static analysis and the second is buckling analysis. The table below shows the characteristics of the pipeline.

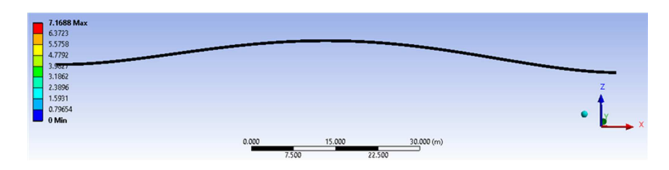


Figure.3: Maximum Deformation (100m free span)

The analysis shows that the maximum deformation is 7.1688m at the middle of the pipeline. This analysis is carried out for 100m free span. As we can see the maximum deformation is quite high. Therefor a shorter free span is considered to decrease the maximum deformation.



Figure.4: Maximum Deformation (50m free span)

The figure above shows maximum deformation for 50m free span. As can be seen, the value is now 0.4486m only which is considerably lower than for 100m free span. The pipeline will require support on the middle of free span to offset the buckling load.

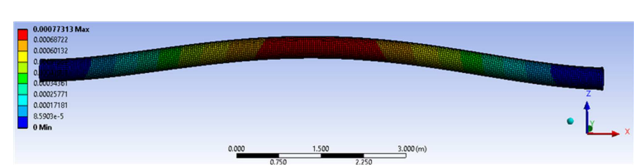


Figure.5: Maximum Deformation (10m free span)

The figure above shows maximum deformation for 10m free

-Science and Engineering-, Vol.1

span. The maximum value is 0.0008 m which is almost zero. This proves that the shorter the free span, the smaller the static deformation. However, selecting the optimum free span must include other factor such as cost and efficiency.

5.0 CONCLUSION

In conclusion, this paper discussed subsea pipeline of Nosong-Bongawan field development, Malaysia. Wall thickness and stress of the subsea pipeline were analyzed using Subsea Pro Simulation and ANSYS. The simulation result shows the simulation result was very close to the actual wall thickness.

ACKNOWLEDGEMENTS

The authors would like to convey a great appreciation to Universiti Teknologi Malaysia and Ocean and Aerospace Engineering Research Institute, Indonesia for supporting this research.

REFERENCES

- 1. Abdul Khair Junaidi, and Jaswar Koto, 2015, *Initial Imperfection Design of Subsea Pipeline to Response Buckling Load*, Journal of Ocean, Mechanical and Aerospace -Science and Engineering-, Vol. 15, pp.7-11.
- Abdul Khair Junaidi, Jaswar Koto, 2014, Parameters Study of Deep Water Subsea Pipeline Selection. UTM Press.
- Abdul Khair Junaidi, Jaswar Koto, 2014, Parameters Study of Deep Water Subsea Pipeline Selection, Jurnal Teknologi, Vol 69, No 7, pp.115-119.
- Abdul Khair, J., Jaswar, Koto, Affis Effendi, Ahmad Fitriadhy, 2015, Buckling Criteria for Subsea Pipeline, Jurnal Teknologi, Vol 74, No 5, pp.69-72.
- 5. ASME B16.5, 2013, Pipe Flanges and Flanged Fittings.
- DNV RP E305, 1988, On-Bottom Stability Design of Submarine Pipelines.
- 7. DNV RP F103, 2010, Cathodic Protection of Submarine Pipelines by Galvanic Anodes.
- 8. DNV, 1981, Rules for Submarine Pipeline Systems.
- Harun Al-Rashid Bin Azmi, 2013, Conceptual Design for Deep Water Pipeline, Faculty of Mechanical Engineering, Universiti Teknologi Malaysia.
- ISO 15589-2, 2007, Petroleum and Natural Gas Industries, *Cathodic Protection of Pipeline Transportation Systems Part* 2: Offshore Pipelines.
- J.Koto, A.K. Junaidi, 2016, Subsea Pipeline Design & Analysis, Second Edition, Ocean & Aerospace Research Institute, Indonesia & Universiti Teknologi Malaysia.
- 12. PETRONAS Technical Standard, PTS 30.10.73.34, 2012, Design of Cathodic Protection Systems for Offshore Pipelines (Amendments/Supplements to DNV RP F103).
- PÉTRONAS Technical Standard, PTS 31.40.00.20, 2012, Pipeline and Riser Engineering.

The Effect of Flat Plate Theory Assumption in Post-Stall Lift and Drag Coefficients Extrapolation with Viterna Method

Faisal Mahmuddin^{a,*}

^{a)}Marine Engineering Department, Engineering Faculty, Hasanuddin University, Makassar Indonesia

*Corresponding author: f.mahmuddin@gmail.com

Paper History

Received: 25-June-2016

Received in revised form: 28-June-2016

Accepted: 30-June-2016

ABSTRACT

In employing blade element momentum (BEM) method to compute the performance of a turbine propeller, the lift and drag coefficients of propeller element/airfoil are needed. The coefficients are usually obtained from model experiment. Unfortunately, the model experiment can only be conducted for small angle of attack until stall mode. Beyond stall mode, Viterna extrapolation method is commonly used. The method is used to predict the lift and drag coefficients from stall angle to 90°. Beyond that range, besides Viterna method, original flat plate theory assumption can also be adopted. The present study compares the lift and drag coefficients extrapolation using Viterna method and flat plat theory. NACA2415 airfoil shape is used for computation. The computation formulas and procedures are presented and important parameter effect to the coefficients are shown and explained.

KEY WORDS: Blade Element Momentum, Experimental Data Extrapolation, Flat Plate Theory, Lift and Drag Coefficients, NACA2415, Viterna Method.

NOMENCLATURE

AR aspect ratio AoA angle of Attack C_D drag coefficient C_L lift coefficient

 α angle of attack

1.0 INTRODUCTION

One of popular methods to predict the power produced by a wind turbine is blade element momentum (BEM) method. The main advantages of the method are simple formulation, fast computation, and good accuracy results especially for steady state condition. Examples of BEM method application can be found in references (Ceyhan, 2008; Døssing, Madsen, & Bak, 2011; Godreau, Caldeira, & Campos, n.d.; Liu & Janajreh, 2012).

In this method, the propeller blade is divided into several elements/airfoil. Each element is assumed to act independently and has no interaction between them. The forces and moments are computed on each element/airfoil. The total forces and moments are obtained by integrating the forces and moments on each element/airfoil.

Therefore, in order to use the BEM method, each element/airfoil performance in terms of lift and drag coefficients is necessary. The performance is usually obtained by conducting a model experiment. However, the model experiments can only be conducted for small angle of attack (*AoA*) until stall mode. For post stall mode performance, it necessary to extrapolate the data obtained from the model experiment in order to obtain the full 360° data

For obtaining the full polar data, several extrapolation methods can be used such as Bean and Jakubowski correlation, Kirke Correlation, Montgomerie model, Viterna model, etc. (Bianchini et al., 2016). Of the methods, Viterna model is the most common one to be used because it can be implemented more straightforwardly with reliable results.

The Viterna method is used specifically to be implemented to predict the lift and drag coefficients from stall mode to 90° of AoA. For AoA higher than 90° , formulation based on the original flat plate theory can also be implemented.

The present study compares the data extrapolation results computed using Viterna method and original flat plate theory. The computation formulas and procedures of both

implementation methods are presented and important parameter effect to coefficients are shown and explained. For demonstrating the calculation procedures, an airfoil based on NACA2415 shape is used.

2.0 SOLUTION METHOD

In the present study, the Viterna method is used to extrapolate the lift and drag coefficients beyond the stall angle until 90o. Beyond that range, original flat plate theory assumption can also be adopted.

2.1 Viterna Method

The Viterna method, also known as Viterna-Corrigan method, is a data extrapolation method for AoA (a) greater than stall angle (α_{stall}) but less than or equal to 90°. The method was formulated by utilizing flat plate theory (Matthew, 2009). It requires an initial angle with its associated drag and lift coefficients which should satisfy flat plate theory.

The Viterna method is formulated to extrapolate the lift and drag coefficients using the following equation (L. A. Viterna & Janetzke, 1982; L. Viterna & Corrigan, 1982):

$$C_L = A_1 \sin 2\alpha + A_2 \frac{\cos^2 \alpha}{\sin \alpha} \tag{1}$$

$$C_D = B_1 \sin^2 \alpha + B_2 \cos \alpha \tag{2}$$

where

$$A_{1} = \frac{C_{D_{max}}}{2} \tag{3}$$

$$B_1 = C_{D_{max}}(4) A_2 = \left(C_{L_{stall}} - C_{D_{max}} \sin \alpha_{stall} \cos \alpha_{stal}\right)$$

$$B_2 = \frac{C_{D_{stall}} - C_{D_{max}} \sin^2 \alpha_{stall}}{\cos \alpha_{stall}}$$
(6)

 C_{Dmax} is found using aspect ratio (AR) as follows

$$C_D = \Box 1.11 + 0.018AR$$
 (7)

The AR in Eq. (7) can be obtained from BEM method application where finite blade length will affects the flat plate assumption. The chosen value of AR will not affect the results significantly. AR equals to 9-10 can be used for most computations.

For data extrapolation from $\alpha > 90^{\circ}$ to $\alpha < \alpha_{min}$, the calculated values are reflected. The Viterna method does not consider pressure or skin friction distributions; however, by making a few simple assumptions and correction, it is possible to obtain a reasonable estimate from the Viterna method. While the method is not an accurate representation of the true physics, it provides a reasonable estimate and accuracy in early design process.

2.2 Flat Plate Theory

It is known from flat plate theory that for deep stall or high angle of attack region (greater than 20°), the upper surface of the airfoil receives no direct impact from the flow due to flow separation. The condition is consistent with what so-called Newtonian Flow condition. Consequently, the thickness of the airfoil can be neglected. In this deep stall region, lift and drag coefficients are largely independent of airfoil geometry but mainly depends on the blade geometry and aspect ratio (J. L. Tangler, 2004).

Moreover, the flow of lower surface is completely laminar, and its contribution to the overall drag force is very small. Therefore, when the foil in high angle of attack position, the foil will behave like a thin of flat plate.

When assuming that the airfoil behave like a flat plate for deep stall angle, the flow separation effect will exist. Therefore, in order to resolve the flat plate flow behaviour, the stagnation point on the rear side of the airfoil is moved by assuming potential flow theory like behaviour. Based on the principle, the curve of lift and drag coefficients can be described using the following equations (Duquette, 2007; J. Tangler & Kocurek, 2005; Timmer, 2010).

$$C_{t} = 2\sin\alpha\cos\alpha \tag{8}$$

$$C_{\rm p} = 2\sin^2\alpha \tag{9}$$

It can be implied from Eq. (8) and (9) that lift and drag coefficients at $\alpha = 0$ will be zero. This is idealization of the curve and not realistic. Even though not realistic, the theory assumption was found to be a good first-order approximation of lift and drag coefficients (Hoburg & Tedrake, 2009).

2.2 4 (four) Digits NACA Airfoil

 $B_1 = C_{D_{max}} \text{ (4) } A_2 = \left(C_{L_{stall}} - C_{D_{max}} \sin \alpha_{stall} \cos \alpha_{stall}^{-1} \cos \alpha_{stall}^{$ and systematic shapes. Based on the shapes, NACA established the shape nomenclature which is now a well-known standard (Tobergte & Curtis, 2013).

Original NACA airfoil series consists the 4-digit, 5-digit, and modified 4-/5-digit which can be drawn using analytical equations that involve the camber (curvature) of the mean-line (geometric centreline) of the airfoil section as well as the section's thickness distribution along the airfoil length. Later series has included the 6-digit series which are more complicated shapes constructed using theoretical rather than geometrical methods.

The 4-digit series are first family of NACA series airfoil. The first digit specifies the maximum camber (m) in percentage of the chord (c), the second indicates the position of the maximum camber (p) in tenths of chord, and the last two digits provide the maximum thickness (t) of the airfoil in percentage of chord. For example, the NACA2415 airfoil, which is the one used in the present study, means the airfoil has a maximum thickness of 15% (0.15c) with a camber of 2% (0.02c) located 40% (0.4c) back from the airfoil leading edge. By knowing the values of m, p, and t, the coordinates and shape of an airfoil can be computed and drawn.

3.0 AIRFOIL DATA

The computed airfoil shape in the present study is NACA2415. Using the definition of 4 (four) digits NACA airfoil described in the previous section, the shape of the airfoil is drawn and shown in the following figure

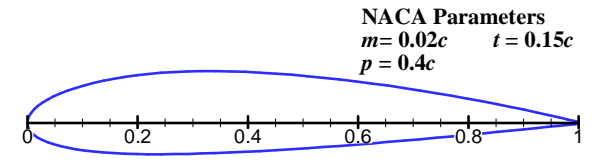
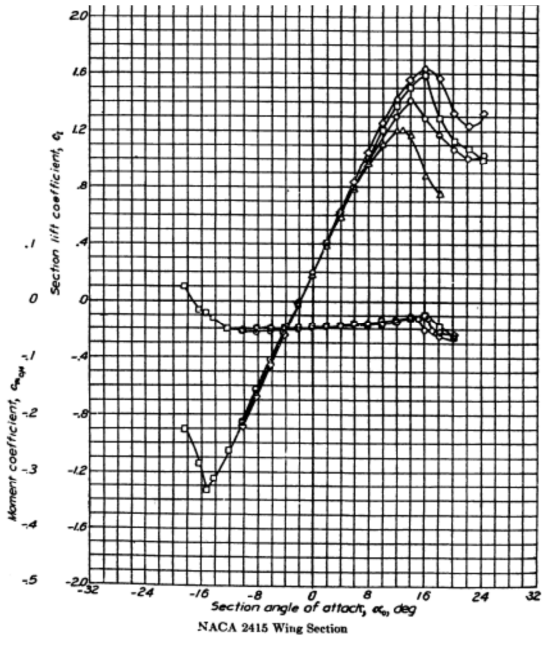


Figure 1: NACA2415 airfoil shape

The lift and drag coefficients of the airfoil will be the input data for the program code. The coefficients of the airfoil will be mostly taken from experiment data which can be found in reference (Abbott & Doenhoff, 1949). The experimental results are shown in the following graphs.



(a) NACA2415 Lift coefficient

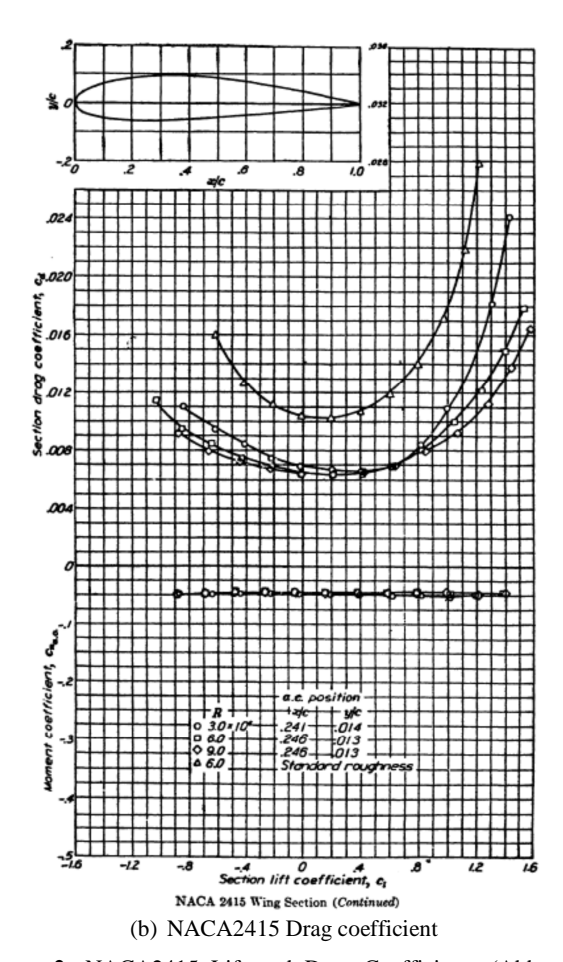


Figure 2: NACA2415 Lift and Drag Coefficients (Abbott & Doenhoff, 1949)

However, it can be seen from Fig. 2 that after AoA of 15.95° , the C_D cannot be determined from experimental graph. Therefore, in order to resolve the issue, a polynomial fit will be used to predict the value of C_D for this range. The same procedure has also been demonstrated in reference (McCosker, 2012).

For the present case, 3^{rd} order polynomial is used to predict the C_D for unknown C_D range. By using the available data, the equation of the polynomial can be determined and shown as

$$8 \cdot 10^{-7} x^3 + 4 \cdot 10^{-5} x^2 + 6 \cdot 10^{-5} x + 0.0063$$
 (10)

The summary of C_L and C_D data obtained from experiment curve and predicted by Eq. (10) are shown in the following table

Table 1: NACA2415 Lift and drag coefficients

Table 1. NACA2413 Efft and drag coefficients					
AoA (degree)	C_L	C_D			
-10.34	-0.86	0.00905			
-8.27	-0.64	0.00786			
-6.2	-0.42	0.00718			
-4.34	-0.24	0.00676			
-2.27	-0.02	0.00647			
-0.2	0.2	0.00648			

20.12

222

24.27

1.87	0.41	0.00651
3.94	0.61	0.00699
5.59	0.84	0.00799
7.66	1.06	0.00935
9.73	1.27	0.01116
11.8	1.43	0.01368
13.66	1.57	0.01613
15.95	1.65	0.019722
18.03	1.59	0.023992

In order to observe more clearly the input data, the data shown in the above table is shown in graph below.

1.34

1.25

1.34

0.029008

0.034766

0.041298

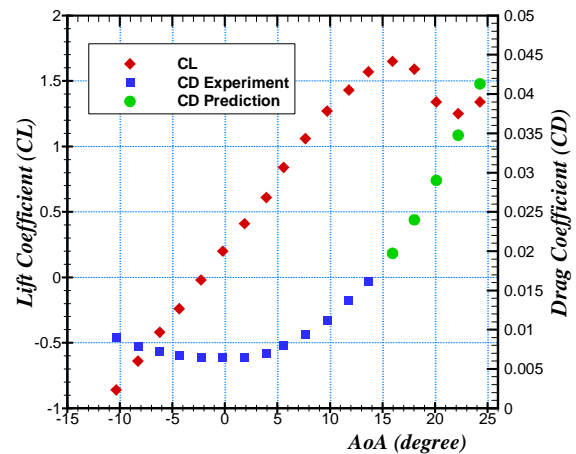


Figure 3: Experimental and predicted C_D and C_L

As shown in the above graph, stall angle is around 15° of AoA. Unfortunately, as described before, the C_D data are not available for post-stall angle. Therefore, they are predicted using polynomial equation shown in Eq. (10). The predicted C_D data are shown as green circle symbol in Fig. 3.

4.0 RESULTS AND DISCUSSION

Based on the airfoil C_D and C_L coefficients shown in Table. 1, computations are performed using the methods described in the preceding section. The first computation is performed to analyse the effect of Coefficient lift adjustment (C_{Ladj}) to lift coefficient. The C_{Ladj} is an important parameter needs to be determined when using the Viterna method to predict the lift and drag coefficients beyond the range from stall angle to 90° . C_{Ladj} will determine the maximum value of computed C_L .

3 (three) values of C_{Ladj} are used which are $C_{Ladj} = 0.7, 0.9$, and 1.2. The computation results are shown in the following figure

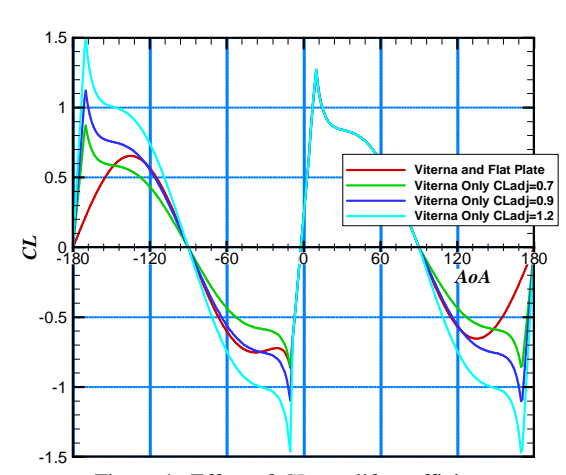


Figure 4: Effect of CL_{adj} to lift coefficient

From figure, it can be seen that $C_{Ladj} = 0.9$ has the best fit to the line compared to other values of C_{Ladj} . Therefore, the next computation will use $C_{Ladj} = 0.9$.

The next computation is performed to analyse the extrapolation of C_L using Viterna method only and flat plate theory assumption. The computation results are shown in the following figure

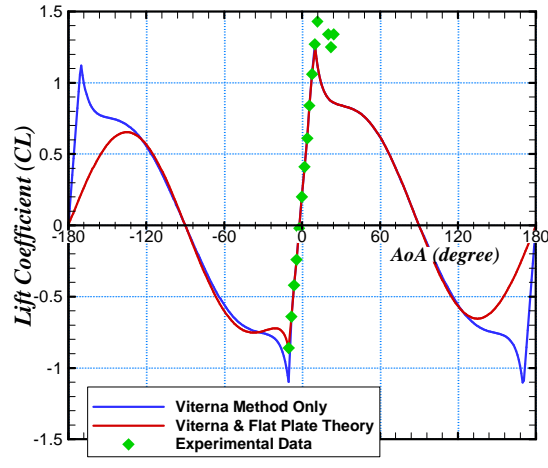


Figure 5: Lift coefficients comparison

It can be observed from the figure that there are discrepancies of results around the peak which are around $\cdot 170^{\circ}$ and 170° . Higher peak can be resolved by implementing flat plate theory assumption as shown as red line. As a result, from the figure, it can also be noted the shape is much more sinusoidal when applying the original flat plate theory assumption. The assumption is used in computing lift and drag coefficients from 90° to 180° and in its reflection in negative side of the curve.

The results for drag coefficients are shown in the following figure

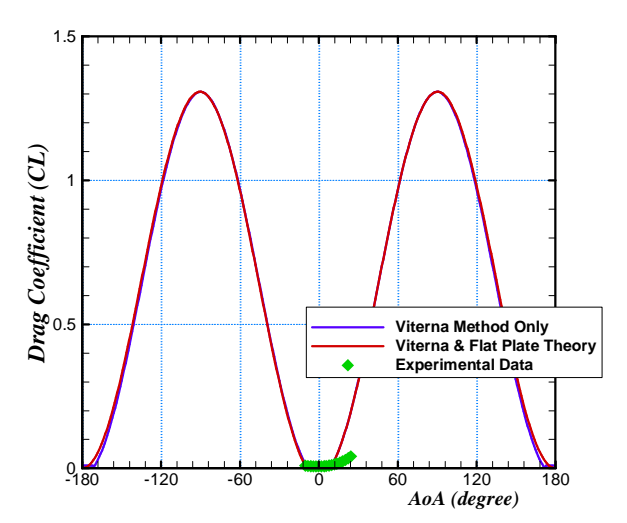


Figure 6: Drag coefficients comparison

From figure above, it can be observed a good agreement between Viterna method and flat plate theory assumption in in terms of shape and magnitude of the curve. The results show that the effect of Viterna method for C_D extrapolation is not significant. Significantly higher C_{Dmax} in the curve can be adjusted using the value of AR as shown in Eq. (7).

5.0 CONCLUSION

In the present study, implementation of lift and drag coefficients experimental data extrapolation using Viterna method and flat plate and theory assumption are performed. It is found that discrepancies can be noticed for lift coefficients while a good agreement can be found in terms of shape and magnitude for drag coefficient. The computation results shown in the present study will be important for determining the Viterna method implementation procedure when using blade element momentum (BEM) method.

ACKNOWLEDGEMENTS

This work was supported by Unggulan Perguruan Tinggi (UPT) research grant from Indonesian Directorate General of Higher Education and Hasanuddin University, Makassar for fiscal year 2016.

REFERENCE

- Abbott, I. H., and Doenhoff, A. E. V. (1949). Theory of Wing Sections Including a Summary of Airfoil Data. New York: Dover Publication, Inc.
- Bianchini, A., Balduzzi, F., Rainbird, J. M., Peiro, J., Graham, J. M. R., Ferrara, G., and Ferrari, L. (2016). An Experimental and Numerical Assessment of Airfoil Polars for Use in Darrieus Wind Turbines Part II: Post-stall Data Extrapolation Methods. *Journal of Engineering for Gas Turbines and Power*, Vol. 138(3), pp: 1–10.

- http://doi.org/10.1115/1.4031270
- 3. Ceyhan, O. (2008). Aerodynamic Design and Optimization of Horizontal Axis Wind Turbines by Using BEM Theory and Genetic Algorithm. Middle East Technical University.
- Døssing, M., Madsen, H. A., and Bak, C. (2011). Aerodynamic Optimization of Wind Turbine Rotors using a Blade Element Momentum Method with Corrections for Wake Rotation and Expansion. Wind Energy, Vol. 15(4), pp: 563–574. http://doi.org/10.1002/we
- Duquette, M. M. (2007). The Development and Application of SimpleFlight, a Variable-Fidelity Flight Dynamics Model. In AIAA Modeling and Simulation Technologies Conference and Exhibit.
- Godreau, C., Caldeira, J., and Campos, J. A. C. F. De. (n.d.). Application of Blade Element Momentum Theory to the Analysis of a Horizontal Axis Wind Turbine. In V Conferência Nacional de Mecânica dos Fluidos, Termodinâmica e Energia (MEFTE). Porto, Portugal.
- Hoburg, W., and Tedrake, R. (2009). System Identification of Post Stall Aerodynamics for UAV Perching. In AIAA Infotech@Aerospace Conference. Seattle, Washington.
- 8. Liu, S., and Janajreh, I. (2012). Development and Application of an Improved Blade Element Momentum Method Model on Horizontal Axis Wind Turbines. *International Journal of Energy and Environmental Engineering*, Vol. 3(30), pp: 1–10
- Matthew, A. B. (2009). A Computational Method for Determining Distributed Aerodynamic Loads on Planforms of Arbitrary Shape in Compressible Subsonic Flow. University of Kansas.
- 10. McCosker, J. (2012). *Design and Optimization of a Small Wind Turbine*. Rensselaer Polytechnic Institute.
- Tangler, J., and Kocurek, J. D. (2005). Wind Turbine Post-Stall Airfoil Performance Characteristics Guidelines for Blade-Element Momentum Methods. In 43rd AIAA Aerospace Sciences Meeting and Exhibit.
- Tangler, J. L. (2004). Insight into Wind Turbine Stall and Post-stall Aerodynamics. Wind Energy, Vol. 7, pp. 247–260. http://doi.org/10.1002/we.122
- 13. Timmer, W. A. (2010). Aerodynamic Characteristics of Wind Turbine Blade Airfoils at High Angles-of-Attack. In *TORQUE 2010: The Science of Making Torque from Wind*. Crete, Greece.
- 14. Tobergte, D. R., and Curtis, S. (2013). Fundamental of Aerodynamics. *Journal of Chemical Information and Modeling*, Vol. 53(9), pp: 1689–1699. http://doi.org/10.1017/CBO9781107415324.004
- Viterna, L. A., and Janetzke, D. C. (1982). Theoretical and Experimental Power From Large Horizontal Axis Wind Turbines (Vol. 82944). Cleveland, Ohio.
- Viterna, L., and Corrigan, R. (1982). Fixed Pitch Rotor Performance of Large Horizontal Axis Wind Turbines. In DOE/NASA Workshop on Large Horizontal Axis Wind Turbines, Cleveland.

Review on Roncador Field Production and Gas Lift Pipelines

Adibah Fatihah.M.Y^a, Noor Zairie. M^a, Nur Ain. A.R^a, Nursahliza. M.Y^a and J.Koto, a,b,*

Paper History

Received: 5-June-2016

Received in revised form: 27-June-2016

Accepted: 30-June-2016

ABSTRACT

The production of oil and gas in Brazil is keeping going as long as there is demand worldwide, same for the development of subsea system technology. The Roncador Field has been leading the technological challenges of Petrobras in ultra-deep water - 1500 to 1900 meters- which covers an area of approximately 110 square kilometers. This paper discussed pressures and stress of subsea pipelines on Roncador Field using Subsea Pro Simulation to analyze the wall thickness and ANSYS to analyze the stress distribution along the pipe.

KEY WORDS: Roncador Field, Wall Thickness, Subsea Pipeline, Stress.

NOMENCLATURE

BBLD Billion Barrels per Day
OD Outside Diameter
ID Inside Diameter
WT Wall Thickness

MMSCMD Million Metric Standard Cubic Meter Per Day

FPU Floating Production Unit EPR Early Production Riser

1.0 RONCADOR FIELD

Campos Basin is located on offshore Rio de Janeiro State, which is on the Southeast region of Brazil. The Campos basin covers area of 100 square km ranging from 20 m to 3,400 m water depth. After Petrobras discovered 2 giant fields in Campos Basin, Albacora, 1984 and Marlim, 1985 in water depth 200 m to 2000 m, they faced 11 years later (1996) to the discovery of Roncador Field in water depth ranging from 1,500 m to 1,900 m. Roncador Field is a giant field located in the northern area of Campos Basin as shown in Figure.1.

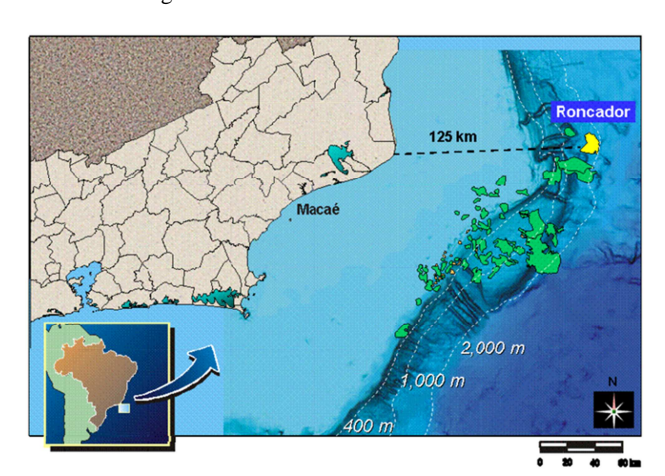


Figure.1: Maps of Campos Basin and Roncador Field [Offshore Energy].

The Roncador Field has been leading the technological challenges of Petrobras in ultra-deep water since it is discovery. It has the world's first drill pipe riser, subsea tree and Early Production Riser (EPR) rated 2,000m. The first well in Roncador is RJS-436A connected to the FPSO Seillean from 1999 to 2001 using EPR at water depth 1,853m with GLL TLD 2000 subsea tree. This field has 3 billion barrels of proven recoverable oil reserves. Due to its large reservoir size, the field was divided into four modules, Module 1 has oil well 28-31 API, Module 2 oil

a) Department of Aeronautic, Automotive and Ocean Engineering, Faculty of Mechanical Engineering, Universiti Teknologi Malaysia

b) Ocean and Aerospace Engineering Research Institute, Indonesia

^{*}Corresponding author: jaswar@utm.my and jaswar.koto@gmail.com

-Science and Engineering-, Vol.6

wells 18 API, Module 3 has oil well 22 API and Module 4 has oil well 18 API. Module 1 has two phases, Phase 1 and Phase 1A. There are total 94 wells in Roncador Field, which is 60 wells are production well and 34 wells are water injection wells. Two types of subsea technologies were used; vertical and horizontal. Both tree technologies are guide-lineless with vertical flow-line connection with individual vertical modules. Several offshore floating structures have been chosen to operate in Roncador Field for production activity such as floating production storage and offloading vessels and semi-submersibles.

2.0 RONCADOR FIELD PROJECT DEVELOPMENT

Petrobras developed Roncador field in four modules because of its large size and different oil gravity in each area. Module 1 has several phases. Figure.2 shows the project development modules in Roncador Field.

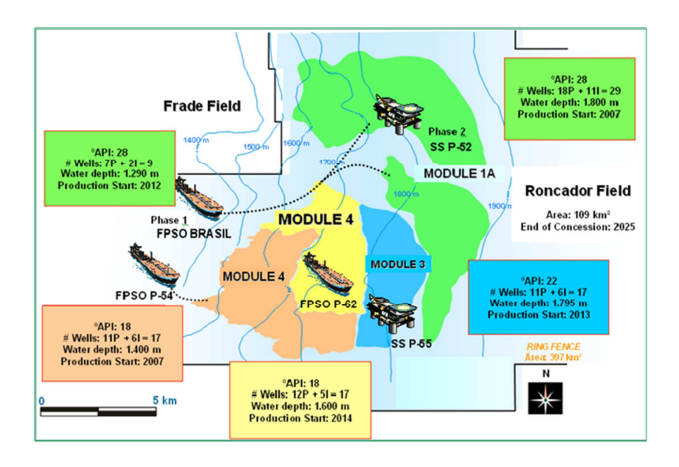


Figure.2: Project Development Modules in Roncador Field [Henrique.at.al, 2013].

The Early Production Phase started producing in 1999 from the first well, RJS-436. This well located at water depth 1,853 m and connected to FPSO Seillean. This phase was set to produce early in order to create revenue for the project to cover the huge costs for development the whole field. During this phase, the production was 20,000 BBLD.

Phase one of Module 1 consisted of several wells connected to semi-submersible production facility P-36. It is start producing in 2000 and later in March 15, 2001, this semi-submersible has sunk due to explosions due to human error. During that time, P-36 is considered the biggest submersible which produced 84,000 BBLD of oil and 1.3MMscmd of processing gas. After the P-36 incident, Petrobras has started with Module 1A: Phase One. They want the field to producing as soon as possible. FPSO Brasil has been installed on water depth 1,290 m and eight production wells have been connected to the vessel. On 2002, the field has started production again.

In Module 1A Phase Two, new build semi-submersible P-52 has been fabricated and installed in 2007. This platform is connected to 18 subsea production wells and 11 water injection wells. The submersible produce 20,000 BBLD peaking to

180,000 in second-part of 2008. The peak gas produced from this phase was 3.2 MMSCMD. For this project, we will focus on Module 1A only. A module 2 development consists of 17 long horizontal wells which 11 of them are production wells and 6 are water injection wells. FPSO P-54 has been assigned for production in this module and started operation in 2007. This phase has helped to boost the overall production from the field to 460,000 BBLD. Development of module 3 consists of 11 add-on production wells and 7 water injection wells. For this module, semi-submersible P-55 has been assigned for production. The production capacity for this platform is 180,000 BBLD and gas compression capacity is 6 MMSCMD. The platform started its production in 2013. Module 4 development consists of 19 wells, which is 12 wells are production well and another 7 wells are water injection well. An FPSO P-62 has been assigned for this module. This FPSO is a cloned to the P-54 FPSO. The production capacity is 180,000 BBLD and gas compression capacity is 6 MMSCMD. This platform started its production in 2014.

3.0 RONCADOR TRANSPORTATION SYSTEM

The module 1A of the Roncador field, offshore Brazil, has been developed employing a large production semi-submersible unit. The integrated gathering system of phase-2 as in Figure.3 involved subseas wellheads and manifold in water depth varying from 1550 to 1900 meters. The production and injection flowlines systems connect the FPU directly to each well, meanwhile the well gas lift flowlines are attached to three subsea manifolds linked to P-52 through a Gas Lift "Ring" pipeline. All flowlines and risers for integrated gathering system are currently both rigid and flexible pipes. Subsea connection flowlines on wellheads and manifolds also were provided by flexible pipe or known as Vertical Connection Module.

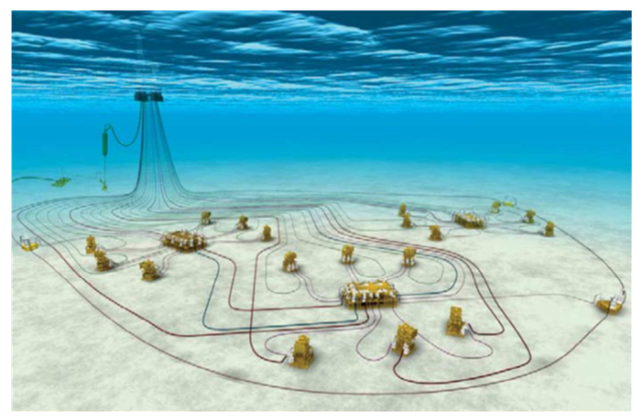


Figure.3: Overview of Roncador subsea system [Claudio, 2014].

These flowlines networks to connect to 18 production wells, 11 water injection wells, 4 spare wells and three manifolds (Jose et al., 2006) consists of 335 km of flexible flowlines for gas and production pipelines and 60 km of rigid pipelines for production and gas lift pipelines. The details for production and gas lift flowline for the respected system as in Table.1.

-Science and Engineering-, Vol.6

Table.1: Production and gas lift flowlines details [Morais et al, 2001].

Particular	Length	Pipe Diameter				
	(m)	(Inch)				
Production pipeline						
Insulated flexible jumper	120	6				
from wellhead						
Insulated steel flowline	8000	6				
with						
PLET's in both ends						
Insulated flexible flowline	1100	6				
Flexible riser to platform	1720	6				
Gas lift Pipeline						
Flexible jumper from	120	4				
wellhead						
Steel flowlines with	8000	4				
PLETs in both end						
Flexible flowline	1100	4				
Flexible riser to platform	1720	4				

In addition, Figure.4 discussed the typical composition of the flowlines which connecting the wellhead to the FPU [Azevedo et al., 2001] consists of:

- 1. Pull in head
- 2. Flange
- 3. Riser
- 4. Extension Flowline
- 5. Isolation Valve
- 6. VCM
- 7. PLET
- 8. Steel Pipeline
- 9. Flexible Jumper
- 10.VCM on Wellhead

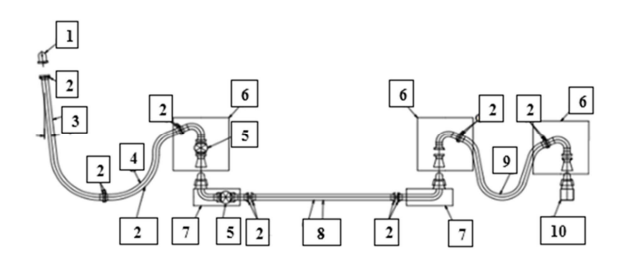


Figure.4: Composition of Flowline [Azevedo et al., 2001].

The production flowlines based on API 5LX60 were coated with fusion-bonded epoxy (FBE) and thermal insulation coating wrapped-solid polypropylene. Gas-lift pipelines based on API 5LX60 were coated FBE-polyethylene for corrosion and mechanical damage protection (single pipeline insulation coating) as in the Table.2: The properties of insulation coating for production pipeline can be described in the Table.3.

Table.2: Roncador Rigid Pipeline Data [Marcos et al., 2001]

Pipeli	ine	Type		Cross Section						
Descrip	ption	of		Steel				Co	ating	
		Steel	OD	WT	ID	OD/WT	FBE	Adhesive	Insulation	Shield
			(mm)	(mm)	(mm)	(mm)	(mm)	(mm)	(mm)	(mm)
6 inch produ	uction line	X60	177.8	14.3	149.3	12.5	0.1	0.4	60	0
4 inch gas lif	ft line	X60	141.3	12.7	115.9	11.1	0.1	0.3	0	5

Table.3: Roncador Production Pipeline Insulation Data [Marcos et al., 2001].

No.	Product	Nominal Thickness (mm)	Thermal Conductivity W/mºK
	Solid Polypropylene	60	0.22

3.0 SUBSEA PIPELINE SIMULATION

3.1 Subsea Production Pipeline

Rocandor field use type single pipe with coating for production pipelines. The pipe consists inside pipe, coating and insulation. Below is the calculation for production pipeline. The pipelines data used in the calculation are shown in Tables.4 - 8.

Table.4: Rigid Pipeline Data

Parameter	Unit	Value
Outside Diameter, D	mm	177.8
Wall thickness, t	mm	14.3
Pipe material grade	-	X60
• Steel Density, $ ho_{st}$	Kg/m ³	7850
Specified Minimum Yield	Mpa	413
Strength, (SMYS)		
Specified Minimum Tensile	MPa	517
Strength, (SMTS)		
• Poisson ratio (v)	-	0.3
Young's Modulus, E	Gpa	207
Thermal Expansion Coefficient (α)	C ⁻¹	1.17x10 ⁻⁵

Table.5: Insulation and Coating Data

Parameter	Unit	Value
Insulation Thickness, t_{cr}	m	0.0001
Insulation Density, $ ho_{cr}$	Kg/m ³	1300
Concrete Coating Thickness, t_{cn}	m	0.060
Concrete Coating Density, $ ho_{cn}$	Kg/m ³	912.2

Table.6: Operating Data

Parameter	Unit	Value
Content Oil density, ρ_{cn}	Kg/m ³	897
Design Internal Pressure, P _i	Mpa	30
Operating Temperature, T_o	°C	67

Table.7: Environmental data

Parameter	Unit	Value
Seawater density	Kg/m ³	1027
Water Depth	m	1870
External Pressure (P_e)	Mpa	18
Ambient Temperature, T_a	°C	5
Friction factor	-	0.58

Table.8: Soil data

PARAMETER VA	LUE

Axial Friction		0.5
Lateral Friction	LB	0.3
	BE	0.5
	UB	0.7
Soil Mobilization		2mm-4mm

The limit state of hydrostatic test pressure can be formulated as follows:

$$P_t \le f_d. f_e. f_t. P_b \tag{1}$$

Where; f_d is burst design factor of internal pressure 0.90 for pipeline and 0.75 for riser, f_e is joint factor of weld and f_t is Temperature derating factor.

Figure.5 shows subsea pipeline stress analysis using Subsea Pro Simulation. The Subsea Pro indicated that the minimum acceptable wall thickness is 14.30 mm for 50 target years. The internal pressure is more dominant at this water depth.









Figure.5: Subsea Production Pipeline Stress analysis using Subsea Pro Simulation.

3.2 Subsea Gas Lift Pipeline

Rocandor field use type single pipe with coating for production gas lift pipelines. The pipe consists inside pipe, coating and insulation. Below is the calculation for gas lift pipeline. The pipelines data are shown in Tables 9 - 11.

Table.9: Rigid Pipeline Data

PARAMETER	UNIT	VALUE
Outside Diameter, D	mm	141.3
Wall thickness, t	mm	12.7
Pipe material grade	-	X60
• Steel Density, ρ_{st}	Kg/m ³	7850
Specified Minimum Yield	Mpa	413
Strength, (SMYS)		
Specified Minimum Tensile	MPa	517
Strength, (SMTS)		
• Poisson ratio (v)	-	0.3
Young's Modulus, E	Gpa	207
Thermal Expansion Coefficient (a)	C ⁻¹	1.17x10 ⁻⁵

Table.10: Insulation and coating Data

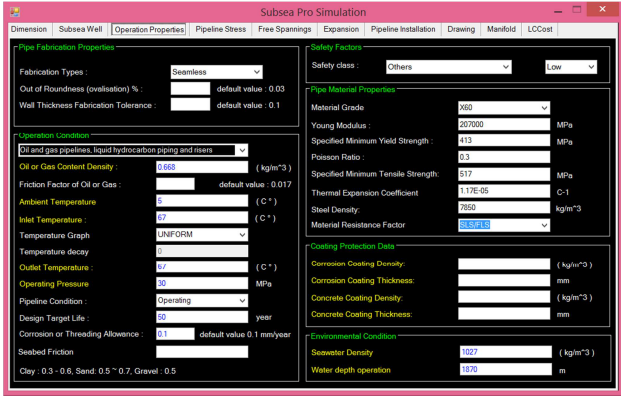
PARAMETER	UNIT	VALUE
Insulation Thickness, t_{cr}	m	0.0001
Insulation Density, $ ho_{cr}$	Kg/m ³	1300
Concrete Coating Thickness, t_{cn}	m	0.005
Concrete Coating Density, $ ho_{cn}$	Kg/m ³	3040

Table.11: Operating Data

PARAMETER	UNIT	VALUE
Content Gas density, $ ho_{cn}$	Kg/m ³	0.668
Design Internal Pressure, P _i	Mpa	30.00
Operating Temperature, T _o	°C	67

Subsea gas lift pipeline stress analysis was done using Subsea Pro Simulation as show in Figure.6. The Subsea Pro indicated that the minimum acceptable wall thickness is 12.43 mm for 50 target years. The internal pressure is more dominant at this water depth.





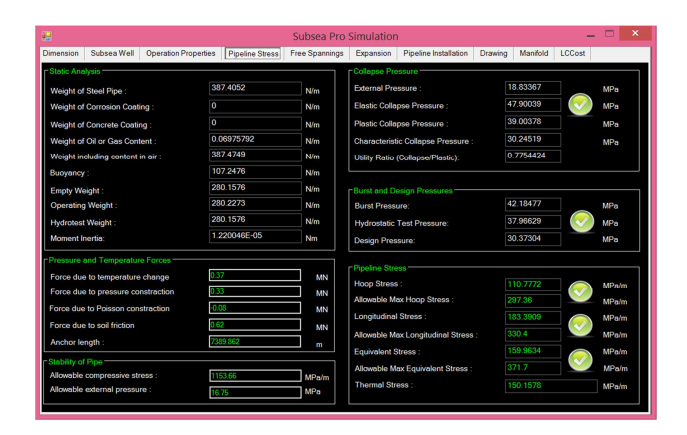


Figure.6: Subsea Gas Lift Pipeline Stress analysis using Subsea Pro Simulation

4.0 FINITE ELEMENT ANALYSIS

Finite element method is a numerical procedure to obtain verification and engineering solutions. The aim for this analysis is to access the structural behaviour of the pipe under loading condition. For this analysis, ANSYS Workbench Static Structural Analysis has been used based on available operating data.

4.1 Load and boundary conditions

In this study, the pipe model is built by ANSYS 14 according to the scale to define stress and strain during normal operation in different water depth level of 1800 meters. The pipe has total length of 120 m and the material properties are correspond to API 5L. The internal pressure of 22 MPa and external pressure of 18 MPa are applied and the wall thickness and outer diameter of pipe for production line are 14.3 mm and 177.8 mm respectively, meanwhile the wall thickness and outer diameter for gas line are 12.7 mm and 141.3 mm respectively (details of the operating condition can be refer at previous section). The both ends of the pipeline are fixed as restraint condition and the simulation is running without pipeline coating.

$\begin{array}{lll} \textbf{4.2 Equivalent stress, strain and buckling for production} \\ \textbf{pipeline} \end{array}$

Figure.5 illustrates the equivalent stress in elastic model without concrete coating by using static structure analysis of ANSYS for production pipe. The maximum stress is 190 MPa while the minimum stress is 79 MPa. The equivalent strain is illustrated by Figure.6 which the maximum 9.6313e-4 and the minimum strain will be 4.7654e-4. Figure.7 show the pipeline buckling for production line which is the maximum deformation is 1.0326 m.

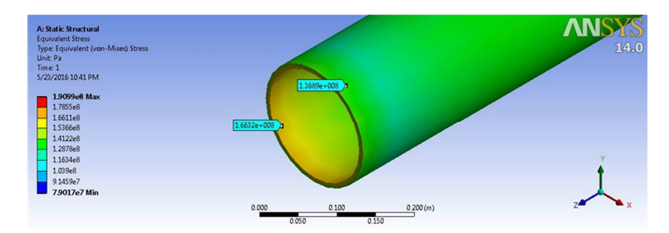


Figure.5: Equivalent stress for production pipeline

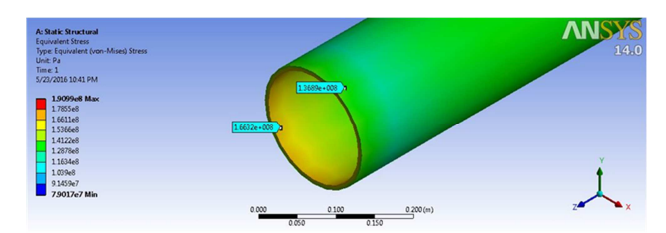


Figure.6: Equivalent strain for production pipeline

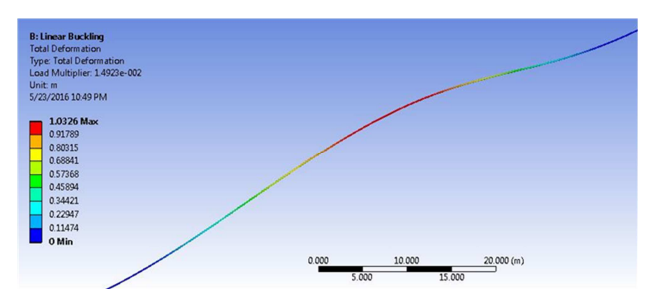


Figure.7: Production Pipeline Buckling In ANSYS Configuration

4.3 Equivalent stress, strain and buckling for gas pipeline

Figure.8 illustrates the equivalent stress in elastic model without concrete coating by using static structure analysis of ANSYS for gas pipeline. The maximum stress is 170 MPa while the minimum stress is 80 MPa. The equivalent strain is illustrated by Figure.9 which the maximum 9.093e-4 and the minimum strain will be 5.244e-4. Figure.10 show the pipeline buckling for production line which is the maximum deformation is 1.0024 m.

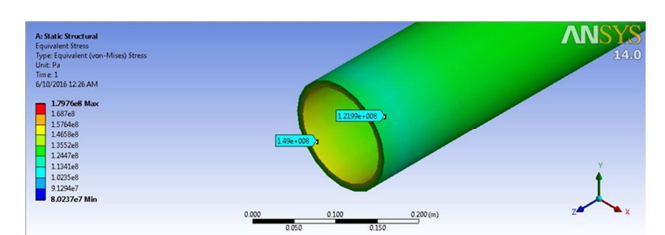


Figure.8: Equivalent stress for gas pipeline

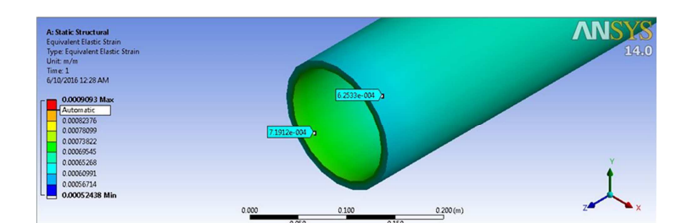


Figure.9: Equivalent strain for production pipeline

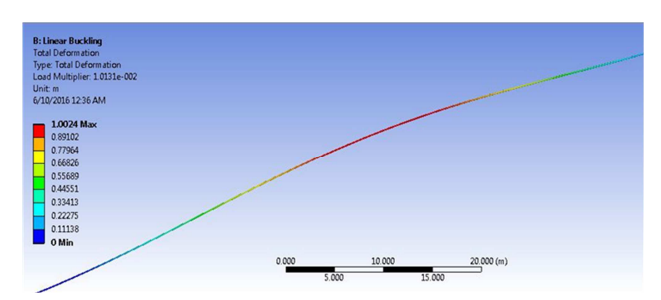


Figure.10: Gas Pipeline Buckling In ANSYS Configuration

5.0 CONCLUSION

In conclusion, this paper discussed on wall thickness and stress of subsea production and gas lift pipelines in Roncador Field, Brasil. Wall thicknesses of the pipelines were investigated using Subsea Pro Simulation and equivalent stress, strain and buckling were analyzed using ANSYS software.

ACKNOWLEDGEMENTS

The authors would like to convey a great appreciation to Universiti Teknologi Malaysia, Malaysia and Ocean and Aerospace Engineering Research Institute, Indonesia for supporting this research.

REFERENCE

- 1. Abdul Khair Junaidi, and Jaswar Koto, 2015, *Initial Imperfection Design of Subsea Pipeline to Response Buckling Load*, Journal of Ocean, Mechanical and Aerospace -Science and Engineering-, Vol. 15, pp.7-11.
- Abdul Khair Junaidi, Jaswar Koto, 2014, Parameters Study of Deep Water Subsea Pipeline Selection, Jurnal Teknologi, Vol 69, No 7, pp.115-119.
- Abdul Khair, J., Jaswar, Koto, Affis Effendi, Ahmad Fitriadhy, 2015, Buckling Criteria for Subsea Pipeline, Jurnal Teknologi, Vol 74, No 5, pp.69-72.
- 4. Bai, Y., & Bai, Q. (2012). Subsea engineering handbook: Gulf Professional Publishing.
- Bordieri, E., Barbosa V. C., Dias, R, 2008, An Overview of the Roncador Field Development, a Case in Petrobras Deep Water Production, Offshore Technology Conference, 5-8 May, Houston, Texas, USA
- 6. Claudio Paschoa, 2014, Brazil Offshore: Petrobras &

- Subsea Engineering, Maritime Professional.
- 7. De Gam Lima, J. M. T., Kuppens, M. L., da Silveira, P. F., and Stock, P. F. K, 2008, Development of Subsea Facilities in the Roncador Field (P-52), *Offshore Technology Conference*, pp. 72 75.
- 8. E. Neto and J. Mauricio, Petrobras S/A and I. Wacleawek, CSO Brazil, 2001, Flexible Pipe for Ultra-Deepwater Applications: The Roncador Experience. "Offshore Technology Conference, Houstan, Texas"
- F.B Azevedo, Petrobras, M. J. B Teixeira, Petrobras, G. Portesan, Soco-Ril, M. Kalman, Garcia, A. L., Pinto, F. J., Dias, M. A., & Mattos, A. M, 1998, Roncador Field-A Rapid Development Challenge in Ultra-Deep Water, Offshore Technology Conference, Houstan, Texas.USA.
- Henrique Peres Moro, Gustavo da Cunha Maia, Daniel Henriques Mesquita Lage and Eduardo Bordieri, 2013, Roncador Module IV: A Successful Case of Heavy Oil Projects in Ultra deep waters, Offshore Technology Conference, Brasil.
- J.Koto, A.K. Junaidi, 2016, Subsea Pipeline Design & Analysis, Second Edition, Ocean & Aerospace Research Institute, Indonesia & Universiti Teknologi Malaysia.
- 12. J.R.F. Moreira and T.E. Johansen (2001). Installation of Subsea Trees in Roncador Field, at 1800m Water Depth Using the Drill Pipe Riser, *Offshore Technology Conference*, Houstan, Texas.
- Jaswar, Abdul Khair, J., H. A. Rashid. 2013. Expansion of Deep Water Subsea Pipeline, *The International Conference* on Marine Safety and Environment, Malaysia
- Jaswar, Abdul Khair, J., Hashif. 2013. Effect of Axial Force Concept in Offshore Pipeline Design. The International Conference on Marine Safety and Environment, Malaysia
- Jose Mauricio T.G Lima, Mariele Lima Kuppens, Paulo Frreira da Silviera, and Pedro Felipe K. Stock, Petrobras (2008). Development of Subsea Facilities in the Roncador Field (P-52). "Offshore Technology Conference Houstan, Texas". OTC 19274
- Juiniti, R, 2001, Roncador Field Development with Subsea Completions, . Conference on Ocean Offshore and Arctic Engineering, Houston, Texas, pp.1-8.
- 17. Keppens, M. L., Batista da Silva, J. L., Ribeiro Contarini, M. G., Pereira Pinto, F. J. C. (2006). Roncador Field Subsea Manifold: A Risk Analysis Approach to Verify the New Installation Procedure. Conference on Ocean Offshore and Arctic Engineering
- Koto, J and Junaidi, A.K, 2016, Subsaa Pipeline Desing & Analysis, Second Idition, Ocean & Aerospace Research Institute, Indonesia.
- L.P. Ribeiro, C. A.S. Paulo and E.A. Neto (2003). Campos Basin- Subsea Equipment: Evolution and Next Steps. "Offshore Technology Conference Houstan, Texas", OTC 15223
- Marcos Morais and Fabio Azevedo, Petrobras / Odd Kvello and Peter Tanscheit, DSND Consub S.A (2001). Deepwater Achievements and Challenges on the Extra Roncador Pipeline Installation Project. "Offshore Technology Conference Houston, Texas, OTC 13258"
- 21. Morais M., Azevedo, F, 2001, Deepwater Achievements and Challenges on the Extra Roncador Pipeline Installation Project, *Offshore Technology Conference*.

- 22. Moreira, C., Pinto, F., Sanches, E., & Brack, M, 2000, Roncador Field Development: The Challenge of the Subsea Hardware Development, *Offshore Technology Conference*.
- Moro, H. P., Maia, G. d. C., Lage, D. H. M., & Bordieri, E, 2013, Roncador Module IV: A Successful Case of Heavy Oil Projects in Ultradeepwaters, Offshore Technology Conference, Brasil.
- 24. Offshore Energy Today, 2012, Brazil: Oil Leak Found at Petrobras' Roncador Field.
- Paula, M. T. R., Labanca, E. L., & Childs, P. 2001, Subsea Manifolds Design Based on Life Cycle Cost, Offshore Technology Conference.
- Ribeiro, M. L. P. G., Segura, M. V. B., Ferreira J. A. N, 2006, Installation Manifold Design for Pendulous Installation Method in Ultra deep water, Conference on Ocean Offshore and Arctic Engineering
- Saliés, J., Nogueira, E., & Evandro, T, 1999, Evolution of well design in the campos basin deepwater, SPE/IADC drilling conference.
- 28. Vilmar Carneiro Barbosa, Ronaldo Dias, 2008, An Overview of the Roncador Field Development, a Case in Petrobras Deep Water Production. *Offshore Technology Conference*, Houston, Texas, USA
- Wellstream, Haliburton, 2001, Deepwater Insulation System for the Steel and Flexible Flowlines of Roncador Field in Brazil. "Offshore Technology Conference Houstan, Texas". OTC 13135.